Journal of Archaeological Science: Reports 24 (2019) 363–372

Contents lists available at ScienceDirect

Journal of Archaeological Science: Reports

journal homepage: www.elsevier.com/locate/jasrep

# Identifying the Roman road from *Corduba* to *Emerita* in the Puente Nuevo reservoir (Espiel-Córdoba/Spain)

Massimo Gasparini[a], Juan Carlos Moreno-Escribano[a], Antonio Monterroso-Checa[b,*]

[a] Project AEI/HAR 77136-R, HUM 882 Research Group, University of Córdoba, Spain
[b] Ramón y Cajal Researcher, Project AEI/HAR 77136-R, University of Córdoba, Spain

ARTICLE INFO

*Keywords:*
Aerial imagery
Photogrammetric acquisitions
Archaeological prospection
Roman road
Roman republican age
Roman imperial age
Endangered heritage
Corduba-Emerita road

ABSTRACT

A stretch of the Roman road between *Corduba* and *Emerita* runs through the modern region of Alto Guadiato in the province of Córdoba (Spain). The structure of this Roman road is well known in the most mountainous part of this territory. However, there are four reservoirs along the course of this road in the flattest part of the region. Therefore, usually the Roman road is submerged and becomes hard to study it. In December 2017 we have been taken advantage of a drought period in order to document the road using remote sensing, photogrammetry and ground investigations. The first step of this research was the identification of this Roman road from several aerial imagery datasets of Spain available in the CNIG. Later, diverse DTM processed from the PNOA LiDAR point clouds were used to obtain the maximum of information in order to design our own photogrammetric acquisitions. Then, we have compared the performance of both photogrammetric DEMs. Finally, this dataset was checked with a ground survey along the Roman road.

In this paper we present the earth observation, remote sensing and ground prospection methods that can be used to study a Roman road in an overall way. Moreover, these resources are very useful when agility is required to get high-quality documentation, as is the case of this submerged stretch of Roman road. Finally, these methods are also helpful to preserve the memory of threated archaeological sites.

## 1. Introduction

### 1.1. Historical significance

The *via Corduba-Emerita* was the only Spanish Roman road that was directly connecting two provincial capital cities: for its situation, it was one of the most important roads at all *Hispania* (Roman Spain). Its Cordovan stretch passes entirely through the modern region of Valle del Alto Guadiato, one of the richest Ancient Spain valleys due to its abundant gold, silver, copper and lead, whose fame even reached Rome. At a certain length along this road, 25 km from its beginning in Córdoba, another significant road begins in a Northeastern direction through Valle de los Pedroches: This second road was connecting Córdoba with *Sisapo*. It was the road that brought the precious minium and mercury extracted in the surroundings of La Bienvenida-Almaden, emperor's property, on its long journey from the port of Córdoba to Rome.

Despite its significance, most of the physic way of this Roman road is not known. We need search it still, because we need understanding better the importance of it structure, considering that armies of Rome, and the merchandise for Rome, passed along this road in ancient times. Here we can show only a stretch of this rich “road of metals”.

To find evidences of this important ancient road, in a wide and relatively unpopulated territory, it is fundamental to take advantage of the huge open-access geographical data made available by the Spanish central administration. It is also important to consider that the area of the Northern province of Córdoba consists in a mountainous zone of very hard accessibility, due to the high slopes, the several agricultural and grazing lands and the presence of wide modern artificial reservoirs that hide territories strongly anthropized in ancient time and that actually can be study only in specific climatic conditions that pass for only short periods and not annually. Once, the evidences are identified, it is necessary to recognize and quickly document these with high detail to preserve the historical and economical information in a territory affected by sudden geomorphological changes, as it is the case study of this paper.

This methodology can be easily repeat in the Spanish territory with a cost-effective result due to, above all, the free geographic data available and it can be also integrated with cheap photogrammetric UAV (Unmanned Aerial Vehicle) platform for more high-detailed

* Corresponding author.
*E-mail addresses:* aa2gagam@uco.es (M. Gasparini), aa2moesj@uco.es (J.C. Moreno-Escribano), amonterroso@uco.es (A. Monterroso-Checa).

https://doi.org/10.1016/j.jasrep.2019.01.026
Received 22 October 2018; Received in revised form 28 January 2019; Accepted 31 January 2019
Available online 08 February 2019

surveys. This workflow is useful not only to identify the route of ancient roads but also to discover archaeological sites (Monterroso Checa, 2017) of different ages and to analyze the evolution of the historical landscape.

### 1.2. Topographical Roman sources. The Iter Cordubam ab Emerita in the Itinerarium Provinciarum Antonini Augusti

The Antonine Itinerary is a collection of most of 220 routes along the roads of the Roman Empire, which dates to the 3rd and 4th centuries B.C. In each case, the beginning and the ending of the route are cited, as well as the route's complete distance in Roman miles. There is also a list of the stops - *civitates* and *mansiones* - along the route while stating the number of miles between each one.

The Antonine Itinerary (as well as another similar road guide from the Roman era: the Ravenna Cosmography) clearly reflects the administrative reality of the Roman Empire, compiling the main routes of each territory and their connection with the main cities. It was used for the orientation of the user while travelling, but it mainly shows the official internal network of the entire empire (Rivet and Jackson, 1970).

In the case of *Hispania*, 34 roads are listed (Roldán Hervás, 2014) with numerous cities along its itinerary. Route 11 corresponds to the *Corduba-Emerita* road (Monterroso Checa and Gasparini, 2016). According to the Itinerary, the distance between Córdoba and Mérida was about CXLIV m.p. (144 miles) and that the cities of *Mellaria*, *Artigis* and *Metellinum* were located between Córdoba and Mérida.

The distance between Córdoba and *Mellaria* is listed as LII m.p. (52 miles), which is roughly equivalent to 77 km. Nowadays, the distance between Córdoba and *Mellaria* is of 85 km by highway. The straight-line distance between Córdoba and *Mellaria* is of 67 km. We have looked for the unknown sections of this Roman road along this distance and we could identify some of them at various locations. The most important is located at the Puente Nuevo reservoir (Fig. 1).

### 1.3. Archaeological background: the via Corduba-Emerita in the Ager Cordubensis by previous investigations

Thanks to the ancient literary and epigraphic sources, as explained in the previous paragraph, it's possible to outline the general path of the road; on the other hand, nowadays minimum stretches of this ancient way are physically known and geographically located in the area of the *Ager Cordubensis*.

The most well-preserved stretch of this way is placed in the so-called “Loma de los Escalones”, 14 km northern of Córdoba, close to the hamlet Cerro Muriano (Melchor Gil, 1995, 116; Monterroso Checa and Gasparini, 2016): here the Roman way is structured as a rock-cut road and it's preserved for approximately 400 m. Another stretch of 30 m of the way is preserved close to the intersection between the country road Espiel – Villaviciosa de Córdoba and the national road 432 at the km 218 (Melchor Gil, 1995, 116). These ones are the most considerable stretches of the Roman way known till today and they sum < 500 m length along a path of 77 km between Córdoba and *Mellaria*.

## 2. Materials and methods

### 2.1. Study area: the Puente Nuevo reservoir in the aerial imagery from PNOA-IGN

Here are compiled by the CNIG all spatial data of Spain acquired by IGN (Instituto Geográfico Nacional – Spanish National Geographic Institute” - https://www.cnig.es/), among others, we can analyze all photogrammetric flights: from the first, the American flight of 1950 (AMS (B) 1956–1957) to recent photogrammetric flights acquired by the PNOA (Plan Nacional de Ortografía Aérea – “National Aerial Orthography Plan”) in 2017 (https://fototeca.cnig.es/). IGN-PNOA is a collection of databases of a major interest to identify and analyses archaeological sites in Spain (Berrocal-Rangel et al., 2017; Blanco-Rotea et al., 2016; Carrero-Pazos et al., 2015; Cerrillo Cuenca, 2017; Cordero


**Fig. 1.** Puente Nuevo reservoir. Situation of the Roman road from *Corduba* to *Emerita*. © OrtoPNOA 2009 CC-BY 4.0 ign.es.


**Fig. 2.** Puente Nuevo Area without the reservoir. Roman road is marked with arrows in the "American flight" AMS (B) 1956–1957 Orthoimage. ©OrtoPNOA-H1956-57 CC-BY 4.0 ign.es.

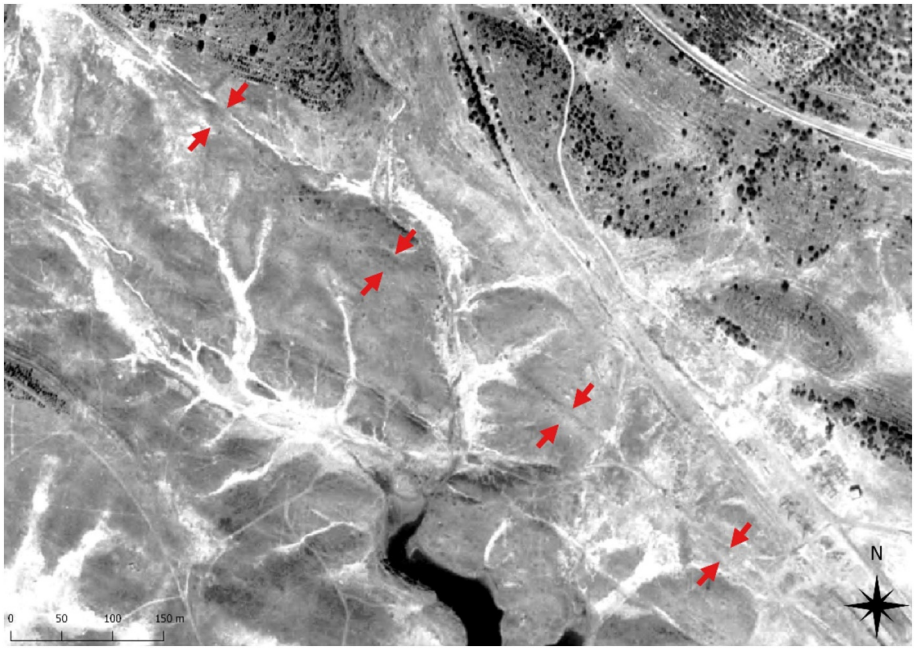


**Fig. 3.** Puente Nuevo reservoir. Roman road is marked with arrows in the "National Flight" of 1980. © FotoN 1980–1986 ign.es CC-BY 4.0 ign.es

Ruiz et al., 2017; Costa-García and Casal García, 2015; Monterroso Checa, 2017; Pérez Álvarez et al., 2013; Vidal Encinas et al., 2018).

The downloaded data regarding to the area of the Puente Nuevo reservoir corresponds to Sheet 0901 of the MTN50 (National Topographic Map 1:50.000).[1]

It was possible to conduct a multitemporal analysis of the evolution of the landscape along this section of the Roman road from Córdoba to Mérida occupied by the Puente Nuevo reservoir with the spatial databases analyzed from 1956 to 2016. We have payed special attention to the years with lower rainfall, as it is the case of 2005, 2007 and 2009.

In the first orthophoto analyzed, the "AMS (B) 1956–1957" (Fig. 2), acquired when the Puente Nuevo reservoir did not exist yet, the road may be discerned clearly. Later, we can recognize and measure with high precision the Córdoba-Mérida Roman road in the photogrammetric flights of 1980 (Fig. 3), 2005, 2007 and 2009 (Fig. 4) due to the low level of the reservoir.

The most interesting file of these aerial imagery collections are belonging to the flight of the PNOA developed in the year 2005. The strong drought occurred in the period of the acquisition of this image

[1] Depending on the selected flight, it consists on orthophotographies in ECW format - with a pixel size between 0.5 and 1 m. with 3 RGB bands – and panchromatic images. The Geodesic Reference system is ETRS89 with UTM projection in Zone 30 with Orthometric height. Each file is accompanied with a Metadata file, with the technical specifications of each photogrammetric flight (López-López and Cerrillo Cuenca, 2016).

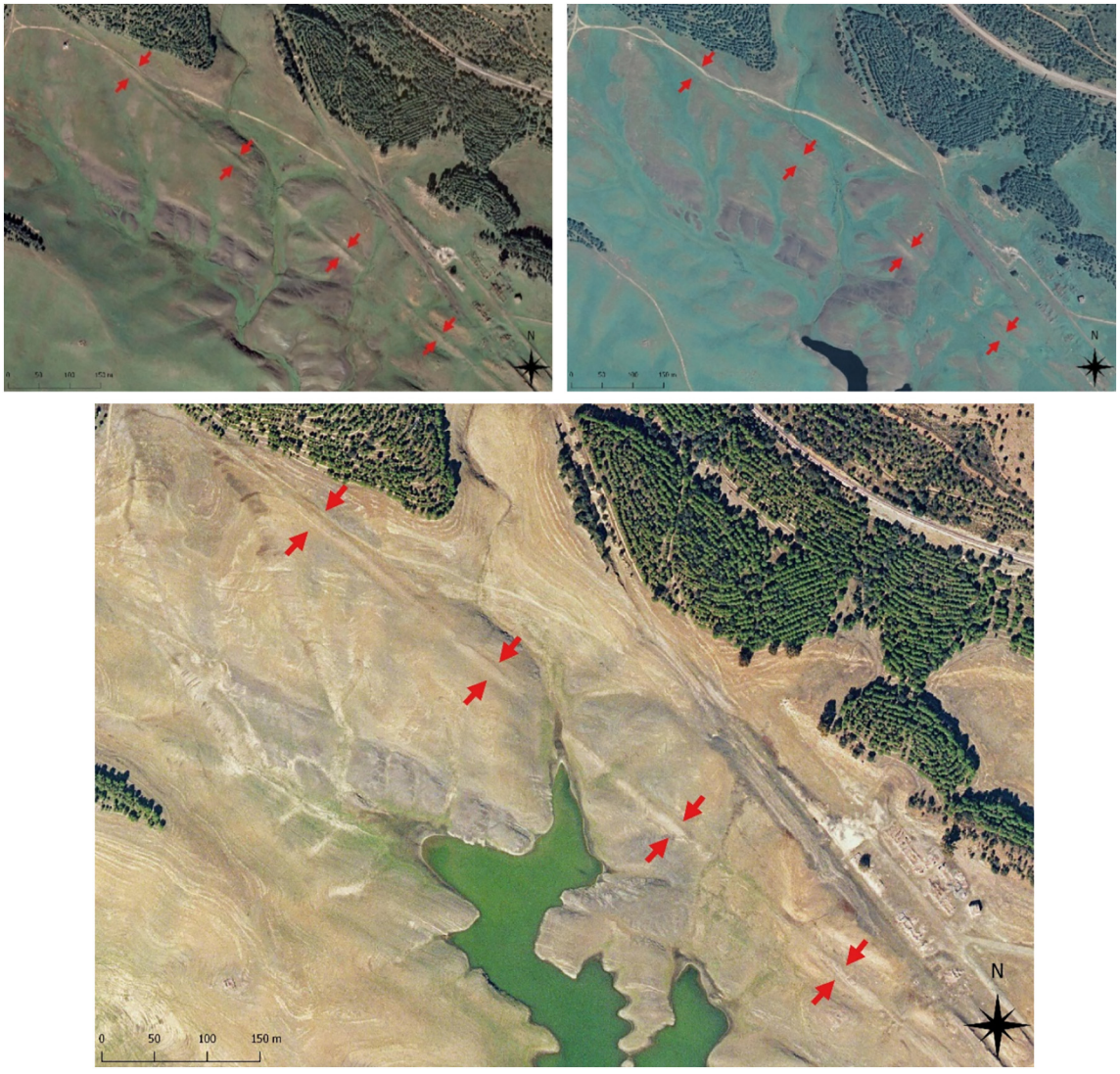


**Fig. 4.** A, B, C. Puente Nuevo reservoir. From the left to the right, from up to bottom, the image shows the localization of the Roman Road in the PNOA Orthoimage of 2007, 2009 and 2005. © PNOA 2005/07/09 ign.es CC-BY 4.0 ign.es.

**Table 1**
Features of Phantom 4 Pro camera used in the acquisitions.

| | |
|---|---|
| Sensor size | 1″ |
| Focal distance | 9 mm |
| Image size | 5472 × 3648 pix |
| ISO speed | ISO-100 |
| Exposure time | 1/200 s |
| Maximum shooting speed | 2 s |
| Capturing system | Image in RGB real colour |
| Image format | JPG |

**Table 2**
Parameters of the first photogrammetric acquisition.

| | |
|---|---|
| Flight height | 20 m |
| Flight speed | 2 m/s |
| Longitudinal overlap | 80% |
| Distance among images (basis) | 4 m |
| Shooting time | 2.13 s |
| Horizontal field of vision | 28.4 m |
| Vertical field of vision | 21.3 m |
| Flight distance | 1240 km |
| Flight time | 11 min |
| Number of photographs | 310 |
| GSD | 0.58 cm |

make it the best one to distinguish the road. It is an orthophoto with RGB bands with a pixel size of 0.5 m. Two parallel lines that run from NW to SE mark clearly the itinerary of the Roman road.

The measurements of this section of the road are 1 km in length and 8 m in width with the coordinates of:

- X: 326460.460 m; Y: 4222639.300 m
- X: 327195.700 m; Y: 4222010.300 m

### *2.2. Photogrammetric acquisitions. Methodology framework, data processing and results*

The optical and photogrammetric flights showed before served us to plan the second methodological step of this work: the acquisition of high detailed photogrammetric survey. The aim of these acquisitions are getting a precise geographical information for the research and planning the future development of excavations.

Using low cost platforms for photogrammetric acquisitions is currently today in many archaeological research projects (Remondino and Nex, 2014), also in Spain (Hernández-Hernandez et al., 2014; Hernández-López et al., 2013; Ortiz et al., 2013; Ruiz Sabina et al., 2015). Normally, the methodologies are very similar, or standardized, when acquisitions are developed along visible archaeological remains.

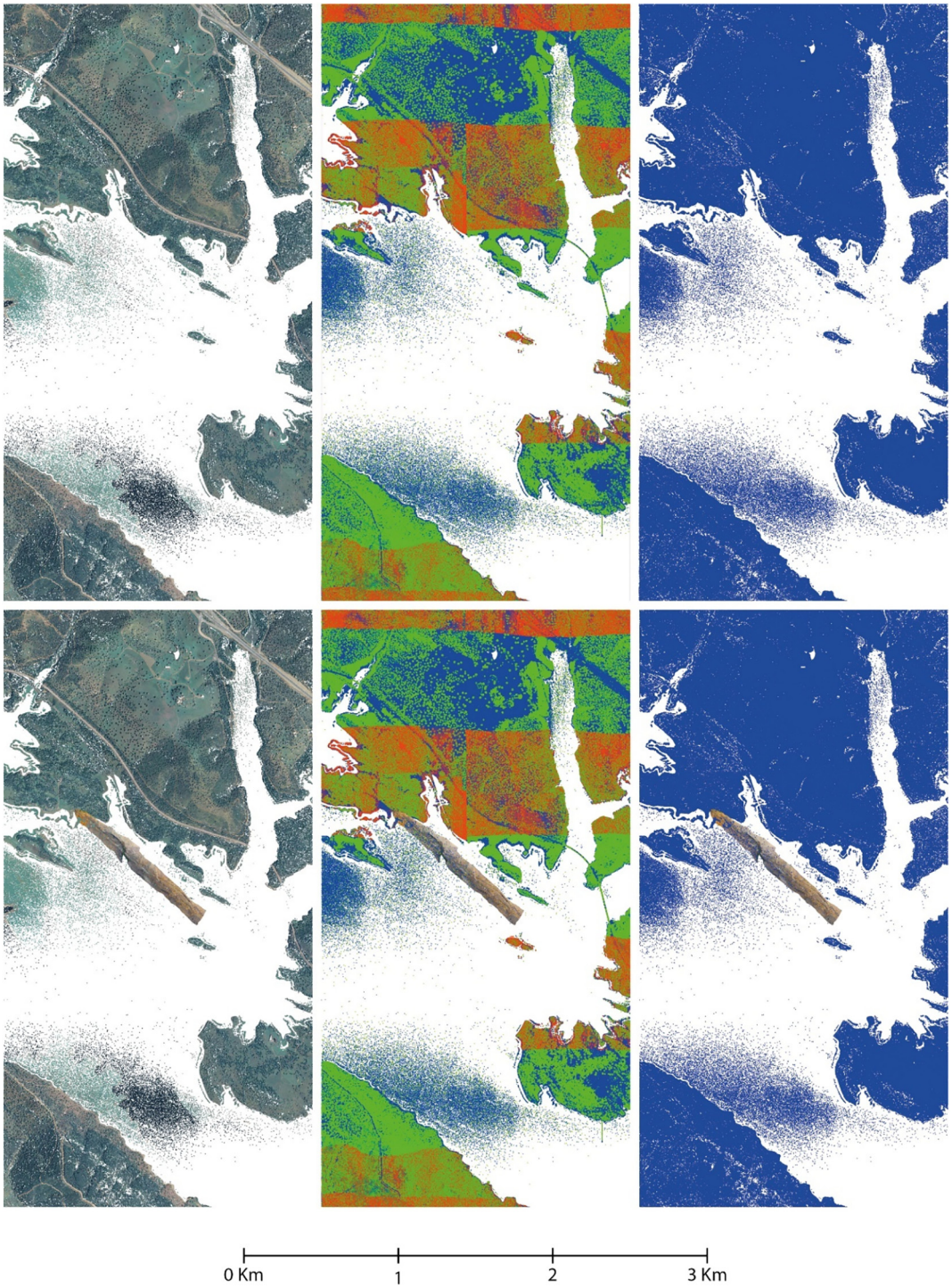


**Fig. 5.** Elaboration of LiDAR and photogrammetric data in CloudCompare (https://www.cloudcompare.org). From the left to the right, from up to the bottom: LiDAR points cloud with RGB data; LiDAR points cloud classified automatically by the IGN; LiDAR points cloud with visible only Class 2 (bare soil) points. It is noted how some points of the swamp water sheet have been recognized as Class 2 points and, therefore, have been used in the interpolation for the creation of the DEM.

However, we want to explain right now our difficulties and goals with the use of these common resources in a very special medium as is an ancient Roman road partially submerged in a reservoir. This is the main goal of this article.

The image-based modelling used was stereoscopic photogrammetry acquired from UAV (Unmanned aerial vehicle) with Structure from Motion post processing (Snavely et al., 2008; Verhoeven et al., 2012) covering the entire road using a DJI PHANTOM 4 PRO drone. The photogrammetric models obtained have been geo-referenced using control points (Targets) and support points (typical stone slabs of the road) whose coordinates have been acquired using GNSS (Global Navigation Satellite System) of dual frequency RTK (Real Time Kinematic) with centimetric precision TOPCON HiPer SR.

The photogrammetric and georeferencing workflow has been carried out through the software Agisoft Photoscan (http://www.agisoft.com).

The shooting settings of the photograms acquired using the drone are the following (Table 1).

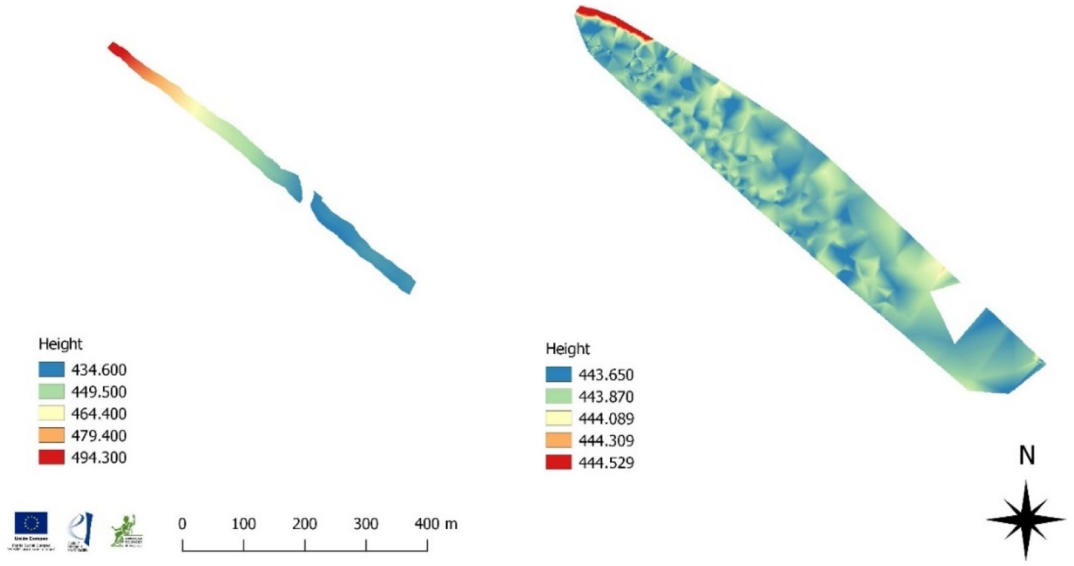


**Fig. 6.** Comparation between DEM processed from the first fotogrammetric acquisitions (on the left) and DEM processed from the LiDAR files of IGN (on the right).

**Table 3**
Parameters of the second photogrammetric acquisition.

| | |
|---|---|
| Flight height | 40 m |
| Flight speed | 3 m/s |
| Longitudinal overlap | 80% |
| Distance among images (basis) | 9 m |
| Shooting time | 2.84 s |
| Horizontal field of vision | 56.9 m |
| Vertical field of vision | 42.7 m |
| Flight distance | 1240 km |
| Flight time | 7 min |
| Number of photographs | 148 |
| GSD | 1.17 cm |

**Table 4**
Features of the point clouds acquired.

| | |
|---|---|
| Average flying altitude | 26.2 m |
| Coverage area | 0.125 $km^2$ |
| Tie point | 340.917 |
| Tie point reprojection | 2.904.821 |
| Root mean square reprojection error averaged over all tie points on all images. | 0,65 px |
| Dense cloud | 210.934.016 |
| GSD (Ground Sample Distance) of orthomosaic | 1.05 cm/px |
| GSD (Ground Sample Distance) of DEM (Digital Elevation Model) | 2.10 cm/px |

The drone flight was programmed to get the best detail available of the characteristics of the road infrastructure. Adapting it to the characteristics of the camera, the flight was planned with the following parameters (Table 2).

After the first acquisition, we must face the problem that in the photogrammetric processing of the data captured, the DEM (Digital Elevation Model) and orthophotos are obtained with a great distortion. The geometry of the only lineal transect acquired is not very strong. Also the photogrammetric point cloud generated is only based on the longitudinal overlap.

The reason is due to the shooting time and the flight height. It is known, that in this drone model, the flight height refers to the point of take-off. As such, if there are increases in the height level of the ground area the flight height shall be < 20 m. With the height between the drone and the ground being lower, the shooting time required among photographs for 80% longitudinal overlap shall be < 2 s, which is not possible with the drone used, due to the minimum time required for taking continuous photographs being 2 s.

To contrast these mistakes, we have compared the DEM obtained with the LiDAR data of the IGN that cover the reference area.[2]

A number of processing methods are available in literature. We have work with QGIS 2.18.19 “Las Palmas” (http://www.qgis.org) and LASTools (https://rapidlasso.com/). The first step has been to process the point-cloud LiDAR files downloaded from de CNIG website through the LASTools tool “blast2dem” (https://rapidlasso.com/blast/blast2dem/). Through the interpolation of the points, this tool allows the creation of a temporary TIN mesh (Triangulated Irregular Network). DEM raster is automatically generated.

Due to the particular conditions in which the section of Roman road is investigated, the most useful product is a DTM (Digital Terrain Model) that has been achieved by interpolating and rasterizing exclusively the points of the LiDAR data classified according to the Class 2, corresponding to the points of the bare soil without vegetation (Fig. 5).

The three images below show the same information acquired from the LiDAR data integrated with the photogrammetric point cloud from UAV. It is very useful to take care of the small area of overlap between the two products available to obtain an accurate comparison of the altimetric data.

Therefore, a series of DTM have been developed from LiDAR data with different spatial resolutions, in order to make a set of altimetric comparisons between these products and the DEMs generated with the same resolution from the points cloud of our photogrammetric acquisitions.

The comparison between both models is focused only in a part of PNOA-LiDAR data from 2014, because this year the reservoir was almost completely full. Only a small, unflooded area, of the 1643 $m^2$ of the northernmost part of the entire study area was able to be compared. The comparison made is the following (Fig. 6).

The left image on Fig. 6 shows the DEM processed after our photogrammetric flight. The red coloured area may reach a height of 494.3 m. However, the model to the right of the Fig. 6 generated with the PNOA-LiDAR data, where in roughly the same area – also coloured

[2] The average point density value of the datasets of PNOA-LiDAR is 0.5 point/$m^2$ in the first coverage (1,4 m between each point) with an altimetric uncertainty of RMSE (Root Main Square Error) ≤20 cm. The Geodesic Reference system is the ETRS89 and the projection used is the UTM in Zone 30. The heights are orthometric. The classification of terrain and off terrain targets from LiDAR acquisition has been made by Instituto Geografico Nacional.

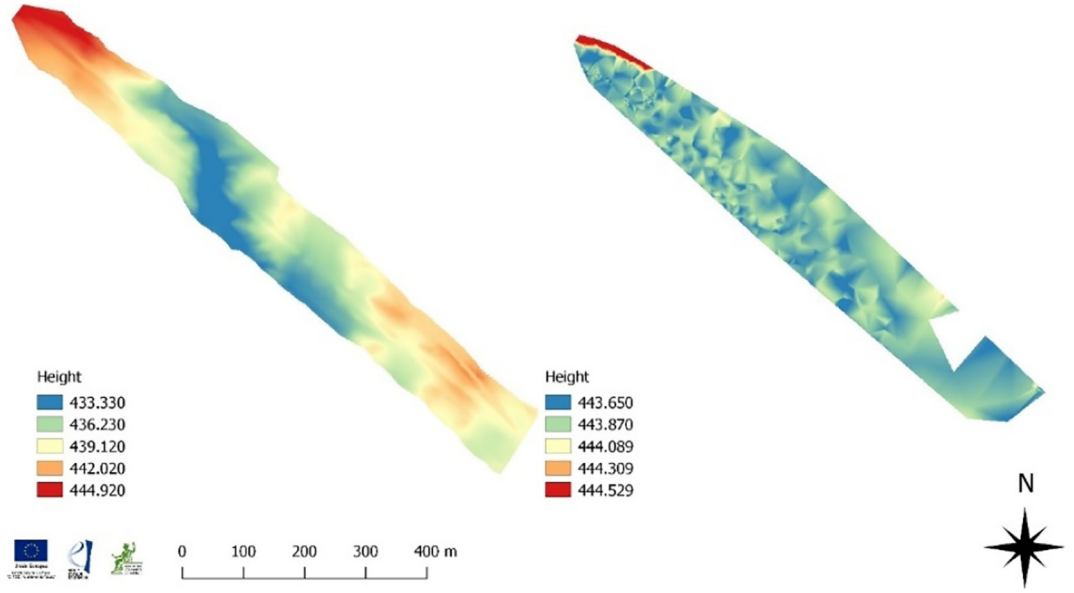


**Fig. 7.** On the left, full DEM as result of the union between the first and the second photogrammetric acquisitions. On the right, DEM processed from the LiDAR files of IGN.

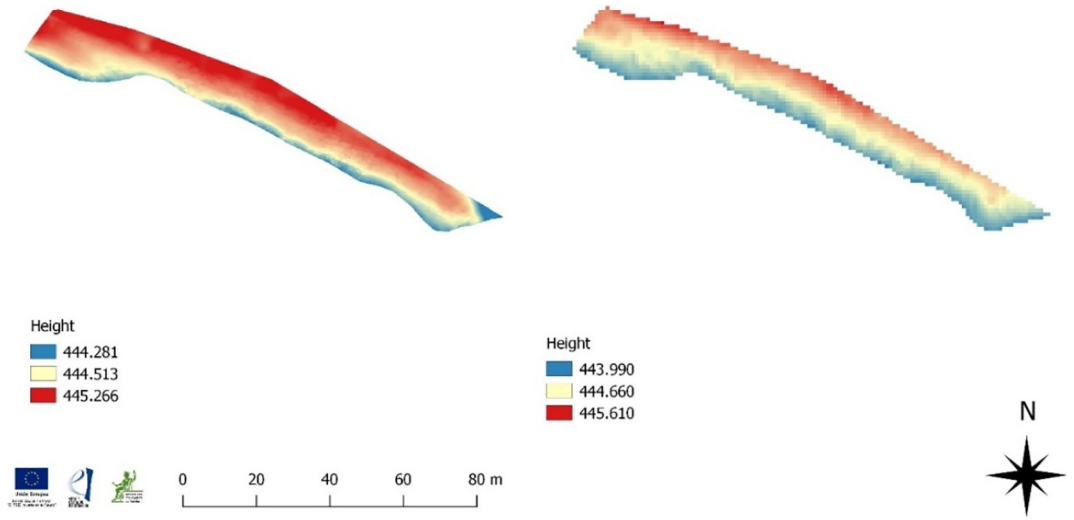


**Fig. 8.** Comparison between our full DEM (on the left) and DEM processed from the LiDAR files of IGN (on the right) in non-cover section of the Roman road.

red – reaches a height of 444.5 m. We have a discrepancy of around 49 m. We should also highlight that a large part of the model obtained in our acquisitions has heights higher than those of the LiDAR data, in which the area flooded by the water (a blue-green coloured area) corresponds to almost all the model. Its height elevation is about 443.8 m; however, the model generated by the flight must be for height values of $< 443.8$ m.

The adopted solution to obtain exacts photogrammetric products has been develop a second lineal flight, with the same alignment, but at a different height. The parameters for the second flight are (Table 3).

The photographs captured were processed with the photographs taken on the first flight. The goal is to assure that an appropriate longitudinal overlap among images with photograph redundancy is achieved. On the other hand, it gives more geometric strength to the photogrammetric flight to get trustworthy results.

The points clouds generated from the union of the photo dataset of the two different flights, georeferenced through the insertion of the GCP taken in the field, offer the following features (Table 4).

The same comparison (Fig. 7) is developed as before (between the LiDAR data of the IGN and the DEM obtained after processing the two flights together). The comparison completed is:

Focusing only on the non-flooded area (red-coloured area) of the model generated with PNOA-LiDAR data, we can assure that the height values are very close to those generated by the UAV acquisitions (Fig. 8).

To make a comparison as close as possible we have generated both DEM with the same parameters (although both the pixel size and the type of interpolation used to rasterize the dense cloud of points affect the altitude values of each of the cells of the DEM).

We have established that the pixel size is the minimum possible (in this case 1 m, since the LiDAR data does not allow a smaller size). The interpolation method used is the irregular triangular network TIN, which uses the algorithms when generating the DEM raster. The algorithm used for the LiDAR data is blast2dem from LAStools for QGIS. The construction of the DEM for the data acquired by aerial photogrammetry has been processed with Agisoft Photoscan (Fig. 9).

Calculating the discrepancies between the altitude values (Fig. 10) there are red and orange pixels with values between $-57$ and $-78$ cm.

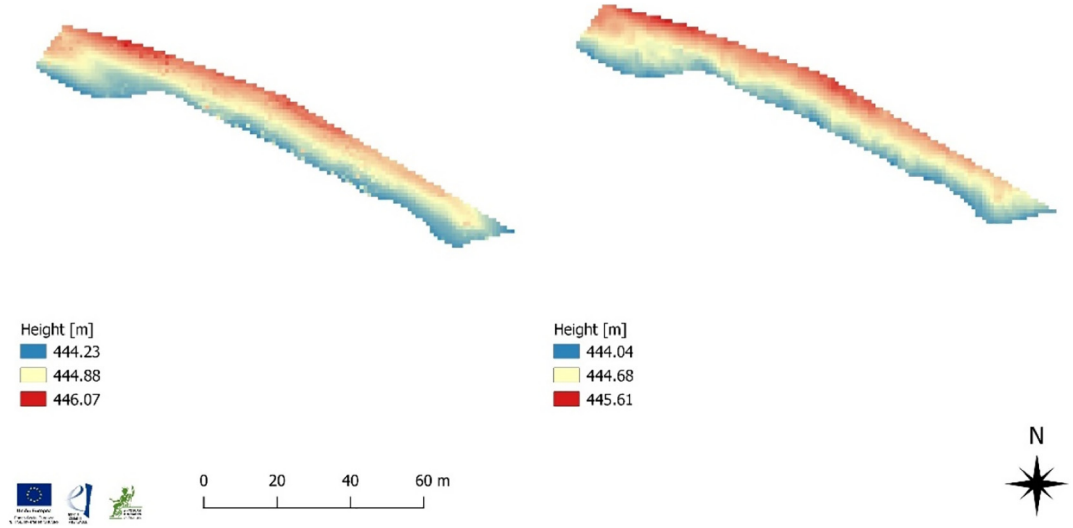


**Fig. 9.** Detail of the comparison between our full DEM and DEM processed from the LiDAR files of IGN (on the right) in non-cover section of the Roman road.

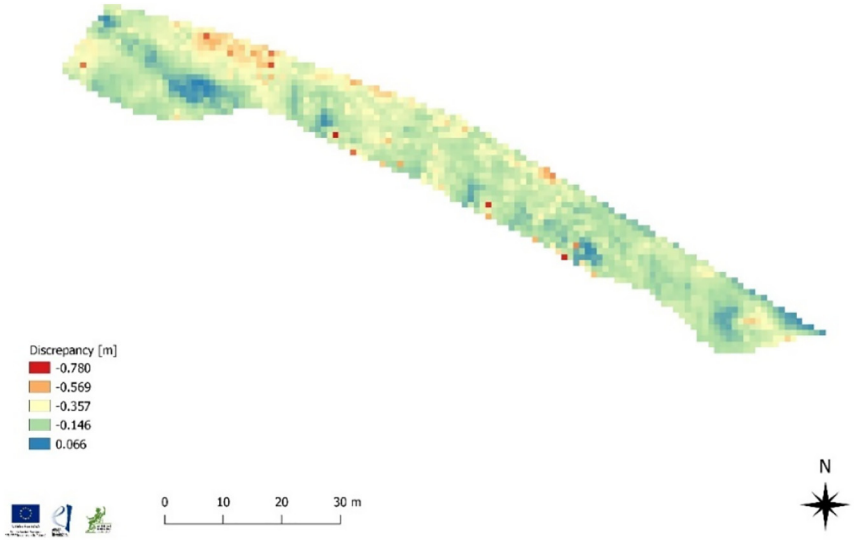


**Fig. 10.** Discrepancy between LiDAR IGN files and our full DEM.

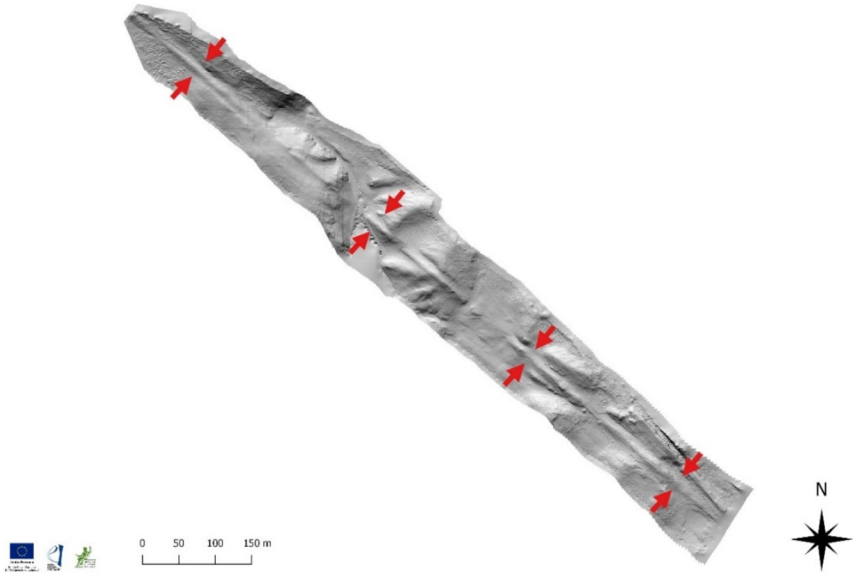


**Fig. 11.** Roman road in the final hillshade of our full DEM.

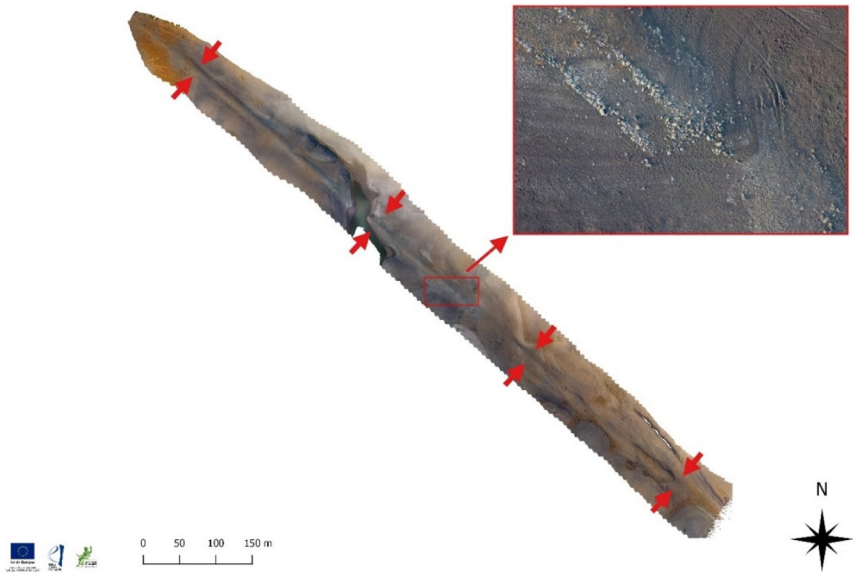


**Fig. 12.** Final Orthoimage with detail of the Roman Road.

**Fig. 13.** Conserved sector of the Roman road from *Corduba* to *Emerita*. The photogrammetric acquisitions developed have captured the original semi-circular mound of mud, small stones and clay of the surface.

**Fig. 14.** The infrastructure under the pavement, shows two lateral walls and one axial wall, captured in the photogrammetric acquisitions.

Although they are high values, they are really few pixels distributed by the terrain, which generally corresponds (above all, the colour orange) with areas where there are trees. The colours shown in most of the terrain correspond to green and yellow, whose values are between −14 and − 36 cm. Finally, in the areas in blue the minimum discrepancies values are of 6 cm.

These discrepancies are considered tolerable because the LiDAR data has an uncertainty of ≤20 cm. Although the maximum discrepancies values are close to 78 cm, the fact that this area only occupy few pixels allow us consider them as residual values from some noisy points or residual values of vegetation in the area. The values that we can consider tolerable, between 6 and −36 cm, cover > 90% of the area. The combination of both flights is considered finally correct as well as the photogrammetric products generated (Figs. 11, 12).

### 2.3. Ground research

We have prospected the entire stretch of the Roman road analyzed in the photogrammetric flights. The structure of this stretch has all the characteristics that a Roman road should have (Mateazzi, 2009), showing the same construction techniques of other well-known Roman roads located in nearby places of Córdoba (Melchor Gil, 1993), Spain and Europe (Moreno Gallo, 2013) (Figs. 13, 14).

In the case of the Roman road of Puente Nuevo reservoir the infrastructure was built excavating different stretches of a large plot of land that was > 12 m wide and 1.5 m deep. Later, also in stretches, two containment walls were inserted on each side on both margins of the road, as is regular for Roman roads.

In this case, a third wall has been built right in the longitudinal center of the road, which divides it into two sections. This was deemed necessary due to the extraordinary width of this road, which has > 8 m of road surface and 12 in total, including the evacuation ditches for water on both sides. Thus, we have two sides that perfectly limit the containment walls.

Once these three longitudinal walls were built in stretches, the surface of the way was filled with different layers of mud and stone. All this makes up the *agger*, or embankment, which is used to build the Roman roads.

Due to this characteristic, the Roman road is recognizable in aerial photographs as well as in our photogrammetric acquisitions.

## 3. Conclusions

We have acquired and compiled a very useful remote sensing dataset may be used in three different ways in the future.

Firstly, we have discovered the location of these sections of the Roman road, which were previously unknown. The high quality georeferenced information acquired allows us to know where the route goes, what its incline is and the orographic difficulties which the Romans faced during its construction.

Also, the photogrammetric documentation allows us to preserve this cultural asset in digital resources "forever". Effectively, these methods of remote sensing allow us to digitally safeguard an endangered heritage, as in this case. It also allows for its scientific dissemination, even though it shall be covered in water again.

Finally, this documentation allows us to plan archaeological excavations with precision when the reservoir's water levels lower again. We already have all the previous documentation required to undertake archaeological surveys in the structure of the road and, therefore, cross-check the information.

Earth Observation, Remote Sensing and Geoscientific Ground Investigations have rescued the memory of an ancient monument from the depths of a reservoir. Now, it is a scientific resource that may be used to recognize the rich heritage of this region along one of the most important roads of the Western Roman Empire.

## Author contributions

Conceptualization, A.M.C.; Methodology, M.G. and JCME.; Investigation, AMC and M.G.; Resources, A.M.C. and JCME; Writing-Original Draft Preparation, A.M.C. and JCME.; Writing-Review & Editing, AMC and M.G. Supervision, A.M.C.

## Funding

This research was funded by AEI-FEDER/Secretaría de Estado de Investigación, Desarrollo e Innovación grant number [HAR 2016 77136-R]. The APC was funded by HUM 882 Research Group-University of Córdoba, Spain.

## Acknowledgments

We thank the anonymous reviewers for their constructive comments. Confederación Hidrográfica del Guadalquivir. Ministerio de Fomento. Gouvernement of Spain.

## Conflicts of interest

The authors declare no conflict of interest.

## References

Berrocal-Rangel, L., Paniego Díaz, P., Ruano, L., Manglano Valcárcel, G.R., 2017. Aplicaciones LiDAR a la topografía arqueológica: El Castro de Irueña (Fuenteguinaldo, Salamanca). In: Cuadernos de Prehistoria y Arqueología. 43. Universidad Autónoma de Madrid, pp. 195–215. https://doi.org/10.15366/cupauam2017.43.007.

Blanco-Rotea, R., Güimil-Fariña, A., Mañana-Borrazás, P., Fonte, J., 2016. Using airborne laser scanning and historical aerial photos to identify modern age fortifications in the Minho Valley, Northwest Iberian Peninsula. In: Kamermans, H., de Neef, W., Piccoli, C., Posluschny, A.G., Scopigno, R. (Eds.), Three Dimensions of Archaeology, Proceedings of the XVII UISPP World Congress, Burgos, Span, 1–7 September 2014 Volume 7/Sessions A4b and A12, pp. 111–120.

Carrero-Pazos, M., Vilas Estévez, E., Romaní Fariña, A., Rodríguez Casal, A., 2015. La necrópolis del Monte de Santa Mariña revisitada: aportaciones del LiDAR aéreo para la cartografía megalítica de Galicia. Gallaecia 33, 39–57.

Cerrillo Cuenca, E., 2017. An approach to the automatic surveying of prehistoric barrows through LiDAR. Quat. Int. 435.B, 135–145. https://doi.org/10.1016/j.quaint.2015.12.099.

Cordero Ruiz, T., Cerrillo Cuenca, E., Pereira, C., 2017. Detección de un nuevo campamento romano en las inmediaciones de Mérida mediante tecnología LiDAR. Saguntum 49, 197–201. https://doi.org/10.7203/SAGVNTVM.49.10025.

Costa-García, J.M., Casal García, R., 2015. Fotografía aérea histórica, satelital moderna y lidar aéreo en algunos recintos militares romanos de Castilla y León. Portugalia Nova Sér. 36, 143–158.

Hernández-Hernandez, J., González-Aguilera, D., Rodríguez-Gonzálvez, P., Mancera-Taboada, J., 2014. Image-based modelling from unmanned aerial vehicle (UAV) photogrammetry: an effective, low-cost tool for archaeological applications. Archaeometry 57 (1), 128–145. https://doi.org/10.1111/arcm.12078.

Hernández-López, D., Felipe-García, B., Gonzáles-Aguilera, D., Arias-Perez, B., 2013. An automatic approach to UAV flight planning and control for photogrammetric applications: a test case in the Asturias Region (Spain). Photogramm. Eng. Remote. Sens. 79, 87–98. https://doi.org/10.14358/PERS.79.1.87.

López-López, A., Cerrillo Cuenca, E., 2016. Arqueología aérea y fuentes de datos libres. Posibilidades y límites. Otarq 1, 181–193. https://doi.org/10.23914/otarq.v0i1.93.

Mateazzi, M., 2009. Costruire strade in epoca romana: tecniche e morfologie. Il caso dell'Italia settentrionale. Exedra 1, 17–38.

Melchor Gil, E., 1993. Vías romanas y explotación de los recursos mineros de la zona Norte del Conventus Cordubensis. AnCord 4, 63–89.

Melchor Gil, E., 1995. Vías romanas de la provincia de Córdoba.

Monterroso Checa, A., 2017. Remote sensing and archaeology from Spanish LiDAR PNOA: identifying the roman the amphitheatre of the roman city of Torreparedones. Mediterr. Archaeol. Archaeometry 2017 (1), 22–56. https://doi.org/10.5281/zenodo.258079.

Monterroso Checa, A., Gasparini, M., 2016. Aerial Archaeology and Photogrammetric Surveys along the roman way from Corduba to Emerita. Digitalizing the ager Cordubensis and the ager Mellariensis. SCIRES-IT 2016 (2), 175–188. https://doi.org/10.2423/i22394303v6n2p175.

Moreno Gallo, I., 2013. Vías romanas. Estado de la cuestión y perspectivas de futuro. Dendra Médica 12 (2), 211–233.

Ortiz, P., Mayoral, V., Mateos, P., Martínez, J.A., Pizzo, A., Liceras, R., de Soto, P., 2013. Analizando el paisaje urbano de Contributa Iulia (Los Cercos, Medina de las Torres, Badajoz), a partir de fotografía aérea de baja altitud. In: Jiménez Ávila, J., Bustamante Álvarez, M., García Cabezas, M. (Eds.), Actas del VI encuentro de arqueología del suroeste peninsular, Villafranca de los Barros, Spain, 4–6 October 2012, pp. 2430–2452.

Pérez Álvarez, J.A., Mayoral Herrera, V., Martínez del Pozo, J.A., de Tena, M.T., 2013. Multi-temporal archaeological analyses of alluvial landscapes using the photogrammetric restitution of historical flights: a case study of Medellin (Badajoz, Spain). J. Archaeol. Sci. 40, 349–364. https://doi.org/10.1016/j.jas.2012.08.025.

Remondino, F., Nex, F., 2014. UAV for 3D mapping applications: a review. Appl. Geomat. 6, 1–15. https://doi.org/10.1007/s12518-013-0120-x.

Rivet, A.L., Jackson, K., 1970. The British section of the Antonine itinerary. Britannia 1, 34–82. https://doi.org/10.2307/525833.

Roldán Hervás, J.M., 2014. Estudio de las vías romanas en Hispania a partir del Itinerario de Antonio, el Anónimo de Ravena y los Vasos de Vicarello. El Nuevo Miliario 17, 10–253.

Ruiz Sabina, J., Gallego Valle, D., Peña Ruiz, C., Molero García, J.M., Gómez Laguna, A., 2015. Fotogrametría aérea por drone en yacimientos con grandes estructuras. Propuesta metodológica y aplicación práctica en los castillos medievales del Campo de Montiel. Virtual Archaeol. Rev. 6 (13), 5–19. https://doi.org/10.4995/var.2015.4366.

Snavely, N., Seitz, S.M., Szeliski, R., 2008. Modeling the world from Internet photo collections. Int. J. Comput. Vis. 80 (2), 189–210. https://doi.org/10.1007/s11263-007-0107-3.

Verhoeven, G., Donesus, M., Briese, Ch., Vermeulen, F., 2012. Mapping by matching: a computer vision-based approach to fast and accurate georeferencing of archaeological aerial photographs. J. Archaeol. Sci. 39 (7), 2060–2070. https://doi.org/10.1016/j.jas.2012.02.022.

Vidal Encinas, J.M., Costa García, J.M., González Álvarez, D., Menéndez Blanco, A., 2018. La presencia del ejército romano en las montañas de El Bierzo (león): novedades arqueológicas. An. Arqueol. Cordobesa 29, 85–110. https://doi.org/10.21071/aac.v29i0.11021.